

Fluorescence Quenching by Sequential Hydrogen, Electron, and Proton Transfer in the Proximity of a Conical Intersection**

Adalgisa Sinicropi, Rebecca Pogni,* Riccardo Basosi, Michael A. Robb, Gabriela Gramlich, Werner M. Nau,* and Massimo Olivucci*

The formulation of a general theory for the control of photon energy disposal by interaction with an external additive stands at the basis of the development of novel fluorescence probes and other photoactive materials. We have shown that the fluorescence quenching of n,π^* -excited states ($X=Y^*$), like aliphatic azoalkanes and ketones, involves hydrogen atom abstraction from the quencher ($R-H$).^[1–3] This abstraction is not completed on the excited state surface but is “aborted” in the region of a conical intersection (CI)^[4] funnel that prompts immediate return to the ground state. This mechanism has recently received support from femtosecond time-resolved experiments in the gas phase.^[5]

In this work, we employ high-level quantum chemical computations^[6–8] and spectroscopic studies of photochemical intermediates to show that the same CI dominates a region of the potential energy surface with exceptional electronic properties, where hydrogen atom, electron, and proton transfer events are interrelated in an uncommon way. In Salem’s correlation diagram for hydrogen abstraction,^[9] an n,π^* -excited state (ES) correlates with the radical pair (RP) derived from *hydrogen atom* abstraction, and the ground state (GS) correlates with the ion pair (IP) derived from *proton* abstraction. Taking into account our previous results,^[1] the originally implicated avoided crossing should be replaced by a CI. The state correlation diagram in Figure 1 is the result. The diagram suggests, implicitly, that a mixture of the ES and GS electronic configurations occurs near the CI where nonadiabatic hops between the ES and GS energy surfaces (vertical dashed arrow in Figure 1) or minute atomic movements on the GS (or ES) energy surface (horizontal dashed arrow) should be accompanied by a sudden change in the electronic configuration from an ES/RP radical-type to a GS/IP covalent/ionic-type wavefunction.

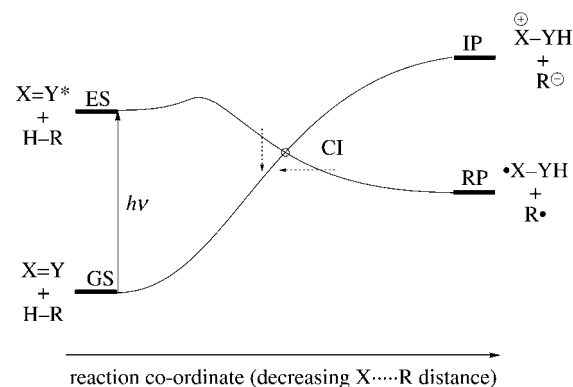


Figure 1. Modified state-correlation diagram of the n,π^* -excited state (ES) correlating with the radical pair (RP) derived from hydrogen atom abstraction and the ground state (GS) correlating with the ion pair (IP) derived from proton abstraction. Note the occurrence of a conical intersection (CI).

The present work was once more performed for n,π^* singlet-excited azoalkanes, which are known to be quenched by hydrogen donors such as chlorinated hydrocarbons and alcohols.^[1,3] The advantage of azoalkanes is mainly an experimental one, since these chromophores, unlike ketones, do not undergo spontaneous intersystem crossing,^[10] which allows a clear-cut assignment of photoreactivity and photo-products to the singlet-excited state, where CIs come into play (in triplet reactions, the CI is replaced by a singlet–triplet crossing).^[11] The pyrazoline/methylene chloride pair was



employed as computational model and the 2,3-diazabicyclo[2.2.2]oct-2-ene (DBO)/chloroform as experimental one. For the computations we have employed ab initio CASSCF, CASPT2,^[12] and MS-CASPT2^[13] calculations to map the minimum-energy paths describing the relaxation from the CI structure and RP disproportionation.^[13–18]

As shown in Figure 2, the CI structure features a 2.01 Å interfragment distance, an almost fully formed 1.02 Å N–H bond, and a planar pyrazoline ring. The result of the wavefunction analysis at the CI shows that GS and ES correlate with IP and RP configurations, respectively, as expected from Figure 1. ES can be formally converted to IP by proton abstraction and to RP by hydrogen atom abstraction. The next efforts were devoted to the characterization of the two distinct relaxation paths corresponding to the vertical and horizontal arrows of Figure 1.

The first path corresponds to “direct” GS reconstitution (light arrows in Figure 2). This involves first S_1 decay by partial hydrogen atom transfer. Upon approaching the CI this process is “aborted” through electron transfer to form a transient ion-pair structure (IP⁺) with a positively charged

[*] Prof. Dr. R. Pogni, Prof. Dr. M. Olivucci, A. Sinicropi, Prof. Dr. R. Basosi
Dipartimento di Chimica dell’Università di Siena
Gruppo di Chimica e Fotochimica Computazionale
Via Aldo Moro, Siena (Italy)
Fax: (+39)0577-234278
E-mail: pogni@unisi.it, olivucci@unisi.it

Prof. Dr. W. M. Nau, Dipl.-Chem. G. Gramlich
Departement Chemie der Universität
Klingelbergstrasse 80, 4056 Basel (Switzerland)
Fax: (+41)61-267-3855
E-mail: Werner.Nau@unibas.ch

Prof. Dr. M. A. Robb
Chemistry Department, Kings College London
Strand London WC2R 2LS (UK)

[**] This work was supported by the Swiss National Science Foundation (project 620-58000.99 for W.M.N. and 2134-62567.00 for G.G.), the Università di Siena (Progetto di Ateneo A.A. 00/02), NATO (CRG 950748), and HFSP (RG 0229/2000-M). We are grateful to Prof. Donati for the use of his monochromator.

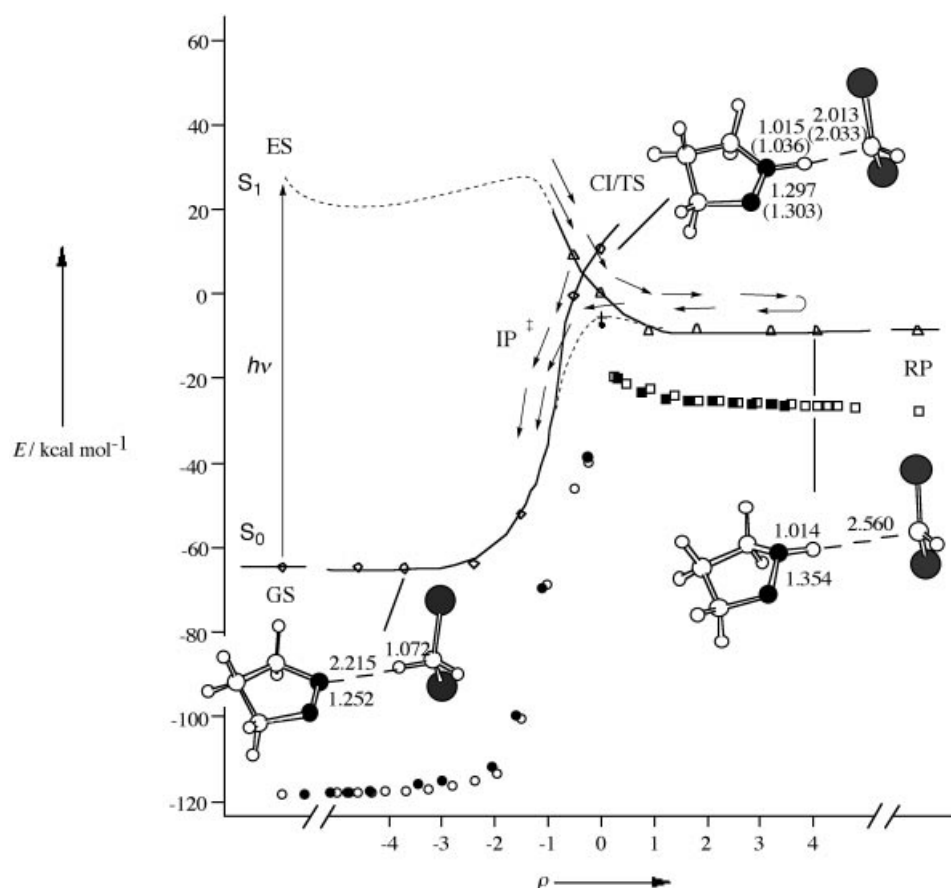
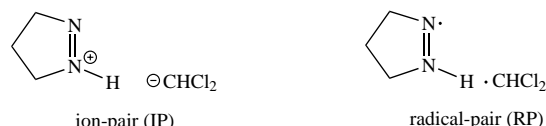


Figure 2. Energy profiles along the CI → GS (CASSCF, ○; CASPT2, ◇) and CI → RP (CASSCF, □; CASPT2, △) relaxation coordinates. The energy profiles of the reactant (CASSCF, ■) and product (CASSCF, ●) branches of the RP → GS reaction coordinate are given together with the corresponding TS energy (CASSCF, ◆; CASPT2, +). The given bond lengths [Å] illustrate the geometric changes occurring along the reaction coordinate ρ [bohr (amu)^{1/2}]; values in parenthesis refer to TS. The energy profile along the initial $^1n, \pi^*$ -path (---) is from ref. [1]; this path corresponds to a different reaction coordinate.

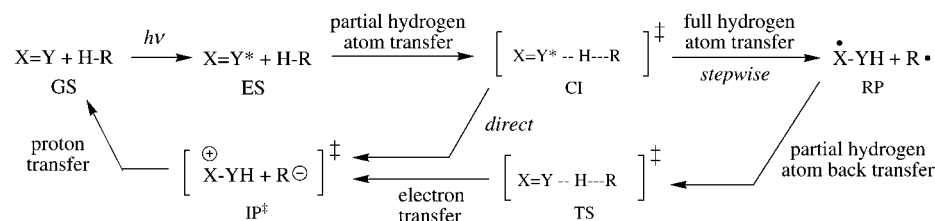


azoalkane fragment (about 0.73 a.u.), 1.1 Å N–H bond, 1.93 Å CHCl₂...H–N distance, and 1.29 Å N–N bond (for example at $\rho = -0.25$ in Figure 2). From IP[‡], proton transfer occurs to reconstitute GS (Scheme 1). Accordingly, the reaction coordinate connecting CI with GS is dominated by N–H expansion and H...C and N–N compression. In

contrast, the second path (full arrows in Figure 2) is dominated by a RP configuration and takes place by a “stepwise” mechanism: radical formation followed by disproportionation to regenerate GS. The corresponding reaction coordinate indicates that RP formation involves an out-of-plane distortion of the azoalkane ring caused by -N-N- expansion and twisting deformation and increased pyramidalization of the N–H center. In detail, the stepwise mechanism can be viewed as a full hydrogen atom transfer followed by a partial hydrogen atom back transfer, an electron transfer (near the CI structure) and, finally, a proton transfer to GS (Scheme 1).

The reaction coordinate for the GS reconstitution by disproportionation of RP has been investigated via a transition-state search on the S₀ potential energy surface. A transition structure (TS) has been located in the strict vicinity of the CI (see geometrical parameters in Figure 2). As reported in Table 1, TS is located about 6 kcal mol^{−1} below the CI and only about 3.5 kcal mol^{−1} (approximately 4.0 kcal mol^{−1} after zero-point

energy correction) above RP. Thus RP disproportionation is expected to be a fast process, competitive with diffusion in solution, which is known to exhibit apparent activation energies for solvent viscous flow around 1–3 kcal mol^{−1}.^[19] The close vicinity of the CI and TS structures and the modest S₁–S₀ energy gap at TS (around 20 kcal mol^{−1}) suggest that the stepwise GS reconstitution involves a S₀ intermolecular electron transfer. The S₀ species, namely the RP intermediate, evolves towards a CI/TS region where an electron jump takes place yielding the same IP[‡] structure as that generated by a direct surface hop at CI. Formally speaking, radical disproportionation does not occur in a simple hydrogen atom transfer step, that is, $^1N-NH + ^1R \rightarrow N=N + HR$ or $RP \rightarrow GS$, but in a stepwise fashion through sequential electron–proton transfer, namely $^1N-NH + ^1R \rightarrow [^1N-NH + ^1R]^{\ddagger} \rightarrow N=N + HR$ or $RP \rightarrow IP^{\ddagger} \rightarrow GS$. This mechanism is consistent with the well-known Polanyi’s harpoon model,^[20, 21] which is usually applied to simple atom plus diatom gas-phase reactions. In our case the mechanism appears to operate



Scheme 1. Intermediates in the fluorescence quenching of n, π^* -excited states ($X = Y^*$) by hydrogen donors ($H-R$) classified according to their dominant electronic structure and the reaction step. The label ‡ indicates unstable transient entities.

Table 1. Calculated energies for the pyrazoline/methylene chloride chromophore/quencher system.

Structure ^[a]	CASSCF <i>E</i> [hartree]	CASPT2 ^[b] <i>E</i> [hartree]	CASPT2 ΔE [kcal mol ⁻¹]
CI (<i>S</i> ₀)	– 1183.89476 ^[d]	– 1185.03836 (0.73) ^[c] { – 1185.04629 }	≡ 0.0
CI (<i>S</i> ₁)	– 1183.89316 ^[d]	– 1185.03768 (0.72) ^[c] { – 1185.02975 }	0.7
GS (<i>S</i> ₀)	– 1183.08361	– 1185.14977 (0.75) ^[c]	– 69.9
RP (<i>S</i> ₀)	– 1183.93902 [0.131] ^[e]	– 1185.06053 (0.74) ^[c]	– 13.9
TS (<i>S</i> ₀)	– 1183.90418 ^[d] [0.132] ^[e]	– 1185.05491 (0.72) ^[c] { – 1185.05503 }	– 10.4
TS (<i>S</i> ₁)	– 1183.88268 ^[d]	– 1185.02138 (0.72) ^[c] { – 1185.02126 }	10.7

[a] For abbreviations, see text, Scheme 1, and Figure 1. [b] The MS-CASPT2 energies (in curly brackets) indicate that the general shape of the energy surfaces is not sensitive to wavefunction mixing. However, as reported for other systems,^[28] a moderate (about 10 kcal mol⁻¹) energy splitting at CI arises due to differences of the optimized MS-CASPT2 CI geometry. [c] The weight of the CASSCF reference function in the first-order function is given in parentheses. [d] State-averaged value (see ref. [14]). [e] Zero-point vibrational energy in squared brackets.

within a more complex organic RP, where the electron-transfer harpoon triggers the following proton transfer. The involvement of a “harpoon” radical disproportionation in a complex fluorescence quenching and the computational manifestation of this mechanistic detail are unprecedented findings, which may be of importance beyond photochemistry in the field of radical chemistry.

To support this conjecture, we have investigated the topological and electronic structure of the CI/TS region in more detail (Figure 3). Figure 3a provides a three-dimensional representation of the energy profiles given in Figure 2. It is evident that the two *S*₀ relaxation paths starting at CI and the two branches of the reaction path defined by TS develop along the same energy valleys. This is demonstrated by the resulting prompt convergence of the relaxation and reaction path branches. Furthermore, vibrational frequency computations along the relaxation paths show that the frequencies associated with the 3*N* – 7 modes orthogonal to the path are all real, thus demonstrating a valley-like structure. To investigate the nature of the *S*₀ wavefunction in the same region, we have computed the *S*₁ – *S*₀ energy gap and fragment charges

along a small loop centered around CI (see dashed circle in Figure 2) and lying along the plane defined by the two modes that lift the *S*₁/*S*₀ energy degeneracy, namely, the branching plane vectors. We start at $\omega = 0^\circ$ with a structure displaced towards IP*. In Figure 3b we show that the charge distribution of the system undergoes two dramatic events. The first event occurs at about 90° and corresponds to a sudden transfer of one electron from the CHCl₂ anion to the pyrazoline cation yielding the RP configuration. The new charge distribution is then maintained up to 270° where a back electron transfer occurs from the pyrazoline radical fragment to the CHCl₂ radical. Notice that the wavefunction changes are associated with the two minima in the energy gap diagram (Figure 3c). It is therefore clear that the *S*₀ energy surface surrounding the CI is divided in two distinct regions with the RP part going from 90° to 270°. Structural analysis reveals that the optimized TS lies on the 90° edge and thus must correspond to the lowest energy critical structure (the bottleneck) for thermal intermolecular electron transfer.

In previous studies^[1–3] on the photoreactivity and quenching mechanism, the actual photoproducts and intermediates

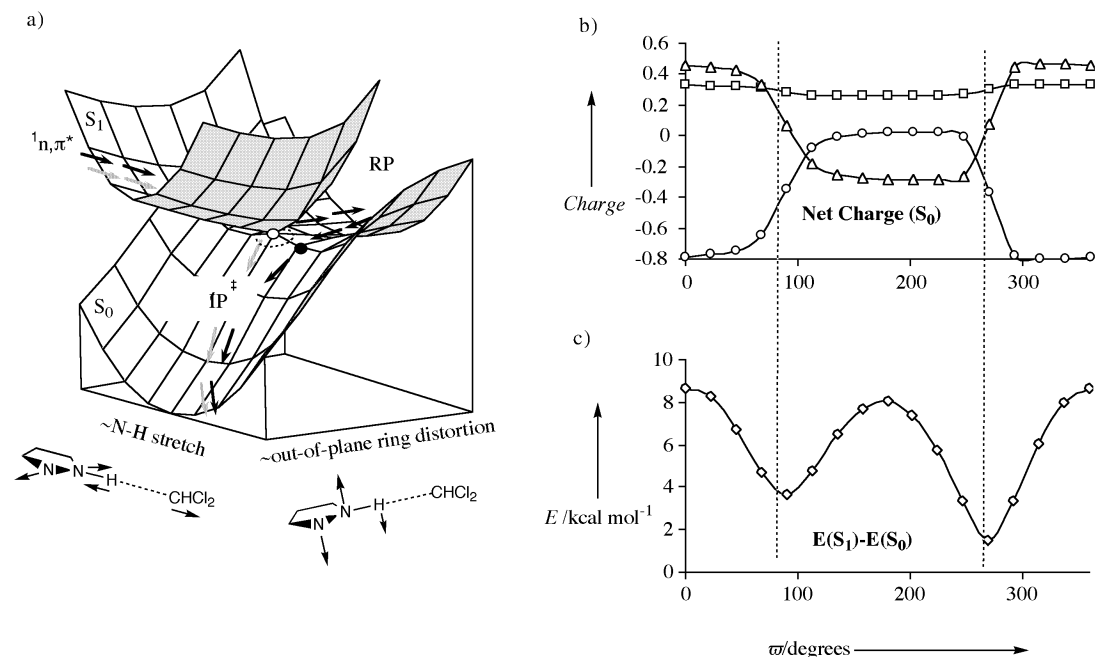
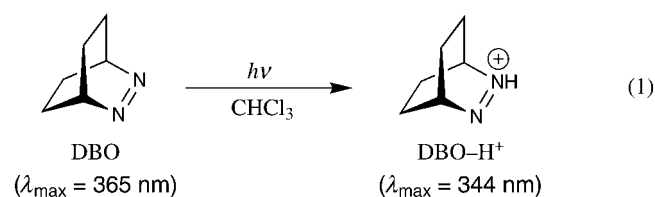


Figure 3. a) Structure of the *S*₁ and *S*₀ potential energy surfaces in the CI/TS region (CI, ○; TS, ●). b) *S*₀ fragment charges [a.u.] along a loop centered around the CI (pyrazoline fragment, △; hydrogen atom, □; CHCl₂ fragment, ○). c) CASSCF *S*₁ – *S*₀ energy gap along the same loop.

were not examined due to the very low photodecomposition quantum yield. However, the above computational findings on the involvement of a metastable RP and a (transient) IP resulting from electron transfer have encouraged a more detailed spectroscopic search for such intermediates. The detection of radicals related to the RP intermediate has been achieved through EPR spectroscopy.^[22] A solution of DBO in chloroform was irradiated at room temperature in the presence of the spin-trap reagent *N*-tert-butyl- α -phenylnitron (PBN). PBN has a high affinity for chlorinated carbon radicals, such as the $\cdot\text{CCl}_3$ radical generated by singlet-excited DBO through hydrogen atom abstraction. The magnetic parameters g (2.0061 ± 0.0001), A_{H} (1.9 ± 0.1), and A_{N} (14.3 ± 0.1) measured shortly after irradiation compare well with the CCl_3 -PBN parameters reported in the literature ($A_{\text{H}} = 1.3$ – 2.9 and $A_{\text{N}} = 13.4$ – 15.5), thus supporting production of the $\cdot\text{CCl}_3$ radical during photolysis.^[23] This radical must derive from hydrogen abstraction with the subsequent formation of the RP intermediate. Although we have provided evidence for the intervention of RP in the photoreaction, no quantitative analysis is possible however, such that we cannot determine to which degree the reconstitution of GS occurs directly through a relaxation from the CI structure (vertical arrow in Figure 1) or through disproportionation of the RP intermediate (horizontal arrow in Figure 1).

In principle, the direct and stepwise pathways for GS reconstitution (see Figure 3a) lead to a *common* unstable IP^+ structure, which regenerates the original GS pair through proton transfer. In contrast to RP, the IP^+ structure resulting from electron transfer is predicted to be unstable, as it immediately accelerates along the proton transfer path. Such a structure cannot be experimentally detected with conventional means. However, our computation neglects the effect of the solvent environment. Solvation could have a significant effect on the shape of the energy surfaces corresponding to the IP^+ state and slow the proton transfer to a degree that ion separation with consequent reactions become competitive.

Circumstantial evidence for the photoinduced formation of ions was indeed obtained. The photolysis of DBO in chloroform^[22] gave rise to the formation of the protonated azoalkane DBO-H^+ with a UV absorption at 344 nm [Eq. (1)],^[24] consistent with the elimination of HCl from the solvent.



This characteristic absorption due to DBO-H^+ could be removed, with a concomitant increase in DBO absorption, upon subsequent addition of triethylamine as a base. Control experiments further revealed that HCl is not formed in the direct photolysis of chloroform (or impurities therein), that is, irradiation of this solvent with subsequent addition of DBO did not produce the characteristic DBO-H^+ absorption. We presume that the trichloromethyl anion serves as an initial

counterion of DBO-H^+ , a process corresponding to a formal proton abstraction. This anion is known to undergo elimination of a chloride anion leading to the overall formation of dichlorocarbene and HCl,^[25] which protonates DBO. Unfortunately, a trapping agent that could intercept dichlorocarbene without quenching the excited azoalkane could not be found, and the complexity of the product mixture prevented further analysis.

Various mechanisms can be invoked to account for the formation of DBO-H^+ . One must recall that a direct proton abstraction of DBO from chloroform is unlikely in view of its negative $\text{p}K_{\text{a}}$ in the excited state^[10] and is also in conflict with the correlation diagram, which precludes a direct correlation with an ionic state (Figure 1). Note also that we have presented evidence by means of deuterium isotope effects^[1–3] and the study of quenchers with varying acidity,^[2] that the quenching is induced by an initial hydrogen atom, and not proton, transfer. We therefore presume, based on the present theoretical findings, that the protonated azoalkane is formed through a sequential hydrogen atom and electron transfer.

In conclusion, the present computational and spectroscopic studies have allowed a detailed mechanistic investigation of the hydrogen abstraction reaction of n, π^* -excited states and the nature of the corresponding conical intersection (CI). This turned out to be unexpectedly rich, since hydrogen atom, electron, and proton transfer all contribute to the same, apparently trivial, quenching process. Most importantly, the disproportionation of the intermediary RP should be better described as a sequential electron–proton transfer (Polanyi's harpooning) in the region of the surface crossing rather than a direct hydrogen transfer. This mechanism, which is inherently related to a surface crossing, may play a role in other radical reactions as well. Also important is the observation that the investigation of electron transfer, which is usually difficult by quantum chemical tools, may become feasible through the investigation of photochemical reaction paths, where mixing of radical- and covalent/ionic-type wavefunctions can be explicitly considered. Recently we have reported examples where different reaction paths for *thermal intramolecular* electron transfer have been successfully mapped.^[26, 27] In this contribution we reported the reaction path mapping for both photoinduced and thermal *intermolecular* electron transfer (the two arrows in Figure 1). Remarkably, in all reported cases electron transfer occurs in the strict vicinity of a CI that thus appears to play a key role for both photochemical and thermal electron transfer.

Received: June 22, 2001 [Z17339]

- [1] W. M. Nau, G. Greiner, J. Wall, H. Rau, M. Olivucci, M. A. Robb, *Angew. Chem.* **1998**, *110*, 103–107; *Angew. Chem. Int. Ed.* **1998**, *37*, 98–101.
- [2] W. M. Nau, G. Greiner, H. Rau, M. Olivucci, M. A. Robb, *Ber. Bunsenges. Phys. Chem.* **1998**, *102*, 486–492.
- [3] W. M. Nau, G. Greiner, H. Rau, J. Wall, M. Olivucci, J. C. Scaiano, *J. Phys. Chem. A* **1999**, *103*, 1579–1584.
- [4] F. Bernardi, M. Olivucci, M. A. Robb, *Chem. Soc. Rev.* **1996**, *25*, 321–328.
- [5] S. De Feyter, E. W.-G. Diau, A. H. Zewail, *Angew. Chem.* **2000**, *112*, 266–269; *Angew. Chem. Int. Ed.* **2000**, *39*, 260–263.

- [6] M. J. Bearpark, F. Bernardi, S. Clifford, M. Olivucci, M. A. Robb, B. R. Smith, T. Vreven, *J. Am. Chem. Soc.* **1996**, *118*, 169–175.
- [7] M. J. Bearpark, F. Bernardi, M. Olivucci, M. A. Robb, B. R. Smith, *J. Am. Chem. Soc.* **1996**, *118*, 5254–5260.
- [8] P. Celani, M. Garavelli, S. Ottani, F. Bernardi, M. A. Robb, M. Olivucci, *J. Am. Chem. Soc.* **1995**, *117*, 11584–11585.
- [9] L. Salem, *J. Am. Chem. Soc.* **1974**, *96*, 3486–3501.
- [10] W. M. Nau, *EPA Newsl.* **2000**, *70*, 6–29.
- [11] M. Klessinger, *Pure Appl. Chem.* **1997**, *69*, 773.
- [12] B. O. Roos, *Acc. Chem. Res.* **1999**, *32*, 137–144.
- [13] J. Finley, P.-Å. Malmqvist, B. O. Roos, L. Serrano-Andrés, *Chem. Phys. Lett.* **1998**, *288*, 299–306.
- [14] Geometry optimization and reaction path computations have been carried out at the CASSCF level of theory using a complete active space including twelve electrons in ten orbitals. The orbitals comprise the π and π^* N=N orbitals, the four σ and σ^* C–N orbitals, the two N lone-pair orbitals of the pyrazoline fragment, and the σ and σ^* orbitals of the reactive C–H bond of CH₂Cl₂. To improve the description of the H transfer, the standard 6-31G* basis set (double- ζ plus d-type polarization functions on first- and second-row atoms) has been augmented with p-type polarization and s-type diffuse functions on the methylene chloride hydrogen atoms and with sp-type diffuse functions included in Gaussian98^[15] on the nitrogen centers. Due to wavefunction instability, the S₀ transition state (TS) has been optimized using state-average CASSCF with a S₀ and S₁ weight of 0.5. The relaxation coordinates have been computed according to the following procedure: a) The CI between the excited state (S₁) and ground state (S₀) was optimized using the methodology available in Gaussian98; b) the S₀ relaxation paths were computed starting from the optimized CI point and using the IRD method described in references [16, 17]. The reaction path branches associated to the optimized TS were computed using the standard IRC method. In order to get a more accurate reaction energetics we re-evaluated the energy along a selected series of relaxation coordinate points using the multireference Møller–Plesset perturbation theory (CASPT2) using MOLCAS-4.^[18] The S₁ and S₀ energies at CI and TS, where the energy gap is small, were re-evaluated using the MS-CASPT2 procedure.^[13]
- [15] *Gaussian98 (Revision A.7)*, M. J. Frisch, G. W. Trucks, H. B. Schlegel, G. E. Scuseria, M. A. Robb, J. R. Cheeseman, V. G. Zakrzewski, J. A. Montgomery, R. E. Stratmann, J. C. Burant, S. Dapprich, J. M. Millam, A. D. Daniels, K. N. Kudin, M. C. Strain, O. Farkas, J. Tomasi, V. Barone, M. Cossi, R. Cammi, B. Mennucci, C. Pomelli, C. Adamo, S. Clifford, J. Ochterski, G. A. Petersson, P. Y. Ayala, Q. Cui, K. Morokuma, D. K. Malick, A. D. Rabuck, K. Raghavachari, J. B. Foresman, J. Cioslowski, J. V. Ortiz, A. G. Baboul, B. B. Stefanov, G. Liu, A. Liashenko, P. Piskorz, I. Komaromi, R. Gomperts, R. L. Martin, D. J. Fox, T. Keith, M. A. Al-Laham, C. Y. Peng, A. Nanayakkara, C. Gonzalez, M. Challacombe, P. M. W. Gill, B. G. Johnson, W. Chen, M. W. Wong, J. L. Andres, M. Head-Gordon, E. S. Replogle, J. A. Pople, Gaussian, Inc., Pittsburgh, PA, **1998**.
- [16] P. Celani, M. A. Robb, M. Garavelli, F. Bernardi, M. Olivucci, *Chem. Phys. Lett.* **1995**, *243*, 1–8.
- [17] M. Garavelli, P. Celani, M. Fato, M. J. Bearpark, B. R. Smith, M. Olivucci, M. A. Robb, *J. Phys. Chem.* **1997**, *101*, 2023–2032.
- [18] *MOLCAS, Version 4*, K. Andersson, M. R. A. Blomberg, M. P. Fülscher, G. Karlström, R. Lundh, P.-Å. Malmqvist, P. Neogrády, J. Olsen, B. O. Roos, A. J. Sadlej, M. Schütz, L. Seijo, L. Serrano-Andrés, P. E. M. Siegbahn, P.-O. Widmark, University of Lund, Lund, Sweden **1997**.
- [19] J. Saltiel, P. T. Shannon, O. C. Zafiriou, A. K. Uriarte, *J. Am. Chem. Soc.* **1980**, *102*, 6799–6808.
- [20] R. D. Levine, R. B. Bernstein, *Molecular Reaction Dynamics and Chemical Reactivity*, Oxford University Press, New York, NY, **1987**.
- [21] M. Polanyi, *Atomic Reaction*, Williams and Norgate, London, **1932**.
- [22] The photolysis experiments were carried out using a 900 W xenon source and high radiance monochromator (Applied Photophysics Ltd) at $\lambda = 380$ nm. For the EPR experiments, fresh chloroform solutions with the spin trap PBN (3 mm) and DBO (6 mm) were thoroughly deaerated with oxygen-free nitrogen for at least 20 min. EPR spectra were recorded at room temperature on a Bruker 200D SRC instrument equipped with a microwave frequency counter XL (Jagmar). The spectrometer was interfaced with a PS/2 technical instrument hardware computer and the data acquired using the EPR data system CS-EPR (Stelar Inc.). Simulations of the EPR spectra were performed using a home-made program. The irradiation in the absence of DBO led to no detectable signal.
- [23] Spin Trap Data Base, NIEHS (National Institute of Environmental Health Sciences) **2001**.
- [24] The formation of protonated DBO upon photolysis of DBO in chloroform was also observed by Feth and Greiner (University of Stuttgart-Hohenheim). We are grateful for this information and related fruitful discussions.
- [25] J. R. Pliego, Jr., W. B. De Almeida, *J. Phys. Chem.* **1996**, *100*, 12410–12413.
- [26] L. Blancafort, F. Jolibois, M. Olivucci, M. A. Robb, *J. Am. Chem. Soc.* **2001**, *123*, 722–732.
- [27] E. Fernández, L. Blancafort, M. Olivucci, M. A. Robb, *J. Am. Chem. Soc.* **2000**, *122*, 7528–7533.
- [28] M. Garavelli, C. S. Page, P. Celani, M. Olivucci, W. E. Schmid, S. A. Trushin, W. Fuss, *J. Phys. Chem. A* **2001**, *105*, 4458–4469.

Molecular Recognition of UDP-Gal by β -1,4-Galactosyltransferase T1**


Thorsten Biet and Thomas Peters*

Dedicated to Professor Joachim Thiem
on the occasion of his 60th birthday

In mammals, protein–carbohydrate interactions play a crucial role in mediating a variety of biological recognition processes.^[1] The enzymes responsible for the biosynthesis of glycan chains are glycosyltransferases, and their malfunction leads to a number of pathological disorders. So far, only limited data are available for the three-dimensional structure of mammalian glycosyltransferases.^[2] Recently, an X-ray structure was published of β -1,4-galactosyl-transferase (β 4Gal-T1, EC 2.4.1.90/38), a Golgi-resident membrane-bound enzyme, in its free and substrate-bound form.^[2c] This transferase is responsible for the transfer of galactose from UDP-Gal (uridine diphospho-D-galactose, Scheme 1) to β -D-N-acetylglucosamine residues, furnishing poly-N-acetylglucosamine chains found in glycoproteins and glycosphingolipids. The enzyme β 4Gal-T1 cocrystallized with the donor substrate UDP-Gal, but the electron density was not sufficient to resolve the terminal galactose residue. Therefore, crucial molecular details of the recognition reaction between β 4Gal-

[*] Prof. Dr. T. Peters, Dipl.-Chem. T. Biet
Institut für Chemie, Medizinische Universität zu Lübeck
Ratzeburger Allee 160, 23538 Lübeck (Germany)
Fax: (+49) 451-500-4241
E-mail: thomas.peters@chemie.mu-luebeck.de

[**] This work was supported by the BMBF (FKZ 031161) and the DFG (Teilprojekt B3 of SFB 470). Financial support from the Verband der Chemischen Industrie is gratefully acknowledged. Dr. T. Keller and Dr. G. Wolff (Bruker Analytik GmbH, Rheinstetten) are thanked for excellent support.

 Supporting information for this article is available on the WWW under <http://www.angewandte.com> or from the author.